SLAC-PUB-17198

Constraints on the Intrinsic Charm Content of the Proton from Recent ATLAS Data

V.A. Bednyakov,[1] S.J. Brodsky,[2] A.V. Lipatov,[1,3] G.I. Lykasov,[1,*] M.A. Malyshev,[3] J. Smiesko,[4] and S. Tokar[4]

[1] *Joint Institute for Nuclear Research, Dubna 141980, Moscow region, Russia*
[2] *SLAC National Accelerator Laboratory, Stanford University, Stanford, CA 94025, United States*
[3] *Skobeltsyn Institute of Nuclear Physics, Moscow State University, 119991 Moscow, Russia*
[4] *Comenius University in Bratislava, Faculty of Mathematics, Physics and Informatics, Mlynska Dolina, 842 48 Bratislava, Slovakia*

Constraints on the intrinsic charm probability $w = P_{c\bar{c}/p}$ in the proton are obtained for the first time from LHC measurements. ATLAS Collaboration data for the production of prompt photons, accompanied by a charm-quark jet in pp collisions at $\sqrt{s} = 8$ TeV are used. Fits to the ATLAS data result in a central estimate: $w = 1.14\%$. Upper limits: $w < 2.74\%$ (4.32%) are obtained at the 68%(95%) C.L. The results, however, do not rule out zero intrinsic charm at one standard deviation. We suggest methods which can reduce the uncertainties for determining the intrinsic charm probability, such as the elimination of theoretical scale ambiguities and tests of $x_T = 2E_T^\gamma/\sqrt{s}$-scaling at fixed rapidity, as well as measurements of the x_T distribution at different LHC energies. Other implications of intrinsic heavy quarks in the proton for QCD studies at the LHC are also discussed.

PACS numbers: 12.15.Ji, 12.38.Bx, 13.85.Qk
Keywords: Quarks, gluons, charm, QCD, PDF

One of the fundamental predictions of quantum chromodynamics is the existence of Fock states containing heavy quarks at large light-front (LF) momentum fraction x in the LF wavefunctions of hadrons [1, 2]. A key example is the $|uudc\bar{c}\rangle$ intrinsic charm Fock state of the proton QCD eigenstate which is generated by $c\bar{c}$-pairs which are multiply connected to the valence quarks. The resulting intrinsic charm distribution $c(x, Q^2)$ is maximal at minimal off-shellness; i.e., when all of the quarks in the $|uudc\bar{c}\rangle$ LF Fock state have equal rapidity. This implies that LF momentum fraction of each constituent is proportional to its transverse mass: $x_i \propto \sqrt{m_i^2 + k_{\perp i}^2}$. The charm quarks in the Fock state thus have a mean LF momentum fraction $\langle x_c \rangle \sim \langle x_{\bar{c}} \rangle \simeq 0.4$. This is in contrast to the momentum distribution of heavy quarks generated at small x_c from perturbative gluon splitting, as predicted by DGLAP evolution. The intrinsic charm probability $w_{c\bar{c}}$ in the proton is typically estimated to be in the 1 to 2% range.

The study of the intrinsic heavy quark structure of hadrons provides insight into fundamental aspects of QCD, especially its nonperturbative aspects. The operator product expansion predicts that the probability for intrinsic heavy Q-quarks in a light hadron scales as κ^2/M_Q^2 due to the twist-6 $G_{\mu\nu}^3$ non-Abelian couplings of QCD [2, 3]. Here κ is the characteristic mass scale of QCD. In contrast, the probability of intrinsic heavy leptons in the Fock state of an atom such as positronium scales as $1/m_\ell^4$, due to the twist-8 $F_{\mu\nu}^4$ light-by-light scattering QED contributions to the atomic self-energy.

There is substantial empirical evidence for intrinsic charm in the proton, starting with the EMC measurements of the charm structure function $c(x, Q^2)$ at large x_{bj} in deep inelastic muon-proton scattering [4]. The charm distribution $c(x, Q^2)$ at $x_c = 0.42$ and $Q^2 = 75$ GeV^2 is found to be roughly 30 times that expected from gluon splitting. A series of ISR experiments measured the production of the heavy baryons Λ_c and Λ_b at high x_F in pp collisions. See, e.g. [5]. The ISR measurements were subsequently verified by SELEX [6] in a series of fixed-target experiments. Intrinsic charm also explains the observation of single and double J/ψ hadroproduction at high x_F by NA3 [7, 8]. In each case, the dissociation of the heavy quark Fock states $|uudQ\bar{Q}\rangle$ of the projectile proton in a high energy collision and the coalescence of the comoving quarks leads to the hadroproduction of hadrons containing heavy quarks at high x_F. Double intrinsic charm Fock states in the projectile hadron also can lead to the hadroproduction of double-charm baryons $|ccq\rangle$ at high x_F [9]. The experimental data for forward Λ_c production at large x_F in pp collision at ISR energies have sizable uncertainties [5, 10]. Moreover, the theoretical description of D-meson, charm and bottom hyperon hadroproduction is sensitive to the fragmentation functions of both c- and u, d-quarks, see [11] and references therein. Therefore, it has been difficult to obtain precise quantitative information on the intrinsic charm contribution to the proton charm parton distribution function (PDF) from the ISR measurements.

In the case of high energy colliders, the intrinsic charm distribution at large x leads to important contributions to the semi-inclusive hard production of prompt photons and gauge bosons accompanied by c-jets from the hard subprocesses $g + c \to \gamma + c$ and $g + c \to Z + c$.

The first indication of this process was observed in the $\bar{p}+p \to c+\gamma+X$ reaction at the Tevatron [12–16]. An explanation for the large rate observed for events at high $E_{\rm T}$ based on the intrinsic charm contribution is given in refs. [17, 18]. A recent review of the experimental results is given in ref. [19]. Recent global analysis of parton distribution fusions (PDFs) with intrinsic charm was presented in [20].

The distribution of intrinsic heavy quarks of the proton involves both perturbative and nonperturbative QCD, since the comoving quarks in the hadron Fock state continually interact.

The intrinsic heavy quark content of the proton can also be determined using lattice gauge theory [21]. The dynamics of interacting comovers will also lead to asymmetries in the heavy quark/antiquark momentum and spin distributions. For example, the matching of the $|uuds\bar{s}\rangle$ Fock state of the proton to its $|K^+(\bar{s}u)\Lambda(uds)\rangle$ hadronic dual leads to $s(x)$ versus $\bar{s}(x)$ momentum and spin asymmetries [22]. The existence of intrinsic heavy quark amplitudes in the B meson can also affect the weak decays of the B meson in an unexpected way [23].

One of the most interesting consequences of intrinsic heavy quark Fock states at the LHC is the novel prediction that the Higgs particle will be produced at high $x_{\rm F} > 0.8$ [24]. This novel process can be used to measure the fundamental couplings of the Higgs to $Q\bar{Q}$ pairs. Intrinsic charm also has important impact for neutrino production from high energy cosmic rays as measured at detectors such as IceCube [25].

In our previous publications [26–29], we showed that the intrinsic charm (IC) contribution in the proton at high $x_{\rm c}$ leads to the production of prompt photons and vector bosons Z/W in pp collisions at the LHC at high transverse momentum accompanied by heavy-flavor c/b-jets. The IC signal in the high transverse momentum spectrum of $\gamma/Z/W$ or the c/b-jets can be significant, especially in the forward rapidity region ($|y| > 1.5$), a kinematic domain within the ATLAS and CMS acceptance. The differential cross section as a function of the photon transverse momentum $E_{\rm T}^{\gamma}$ provides a measure of the intrinsic charm probability w [28, 29].

In this paper we utilize this feature with the goal to estimate the intrinsic charm probability w in the proton. To this end, using the χ^2-method, we minimize the difference between the above-mentioned w-dependent cross section and the ATLAS measured $E_{\rm T}^{\gamma}$-spectra of prompt photons produced in association with c-jets in pp collision at $\sqrt{s} = 8$ TeV [30].

As shown in ref. [26], the subprocess $cg \to \gamma c$ at lowest order in pQCD gives the main contribution to the IC signal in $pp \to \gamma cX$ reaction at large $E_{\rm T}^{\gamma}$ and $|y| > 1.5$, i.e., in the domain where $x_{\rm c} > 0.1$. We have evaluated the production cross section from the IC contribution using the Monte-Carlo (MC) generator SHERPA [31]. The analysis provides MC-generated set of histograms with small steps in w. The goal is to obtain the best description of data and to constrain the intrinsic charm contribution.

The systematic uncertainties due to hadronic structure were evaluated using a QCD approach, based on the $k_{\rm T}$-factorization formalism [32, 33] in the small-x domain and the assumption of conventional (collinear) QCD factorization at large x.

We have employed the $k_{\rm T}$-factorization approach to calculate the leading contributions from the $\mathcal{O}(\alpha\alpha_s^2)$ off-shell gluon-gluon fusion $g^* + g^* \to \gamma + c + \bar{c}$. In this way one takes into account the perturbative charm contribution to associated $\gamma + c$ production. The IC contribution is computed using the $\mathcal{O}(\alpha\alpha_s)$ QCD Compton scattering $c+g^* \to \gamma+c$ amplitude, where the gluons are kept off-shell and incoming quarks are treated as on-shell partons. This is justified by the fact that the IC contribution starts to be visible at large $x \geq 0.1$ a domain where its transverse momentum can be safely neglected. The $k_{\rm T}$-factorization approach has technical advantages since one can include higher-order radiative corrections by adopting a form for the transverse momentum dependent (TMD) parton distribution of the proton (see reviews [34] for more information).

In our analysis we have used the conventional QCD factorization method which provides reliable theoretical predictions for the large-x region. For comparison, we have also used a combination of the k_T and QCD factorization methods, employing each of them in the kinematic regime where it is most suitable.

According to the BHPS model [1, 35], the total charm distribution in a proton is the sum of the *extrinsic* and *intrinsic* charm contributions.

$$xc(x,\mu_0^2) = xc_{\rm ext}(x,\mu_0^2) + xc_{\rm int}(x,\mu_0^2). \qquad (1)$$

The *extrinsic* quarks and gluons are generated by perturbative QCD on a short-time scale associated within the large-transverse-momentum processes. Their distribution functions satisfy the standard QCD evolution equations. In contrast, the *intrinsic* quarks and gluons are associated with a bound-state hadron dynamics and thus have a non-perturbative origin. In Eq. 1 the IC weight is included in $xc_{\rm int}(x,\mu_0^2)$ and the total distribution $xc(x,\mu_0^2)$ satisfies the QCD sum rule, which determines its normalization.

As shown in [28, 29], the interference between the two contributions to Eq. 1 can be neglected, since the IC term $xc_{\rm int}(x,\mu^2)$ is much smaller than the extrinsic contribution generated at $x < 0.1$ by DGLAP evolution [36–38] from gluon splitting. Therefore, since the IC probability w enters into Eq. 1 as a constant in front of the function dependent on x and μ^2, one can adopt a simple relation for any $w \leq w_{\rm max}$:

$$xc_{\rm int}(w,x,\mu^2) = \frac{w}{w_{\rm max}} xc_{\rm int}(w_{\rm max},x,\mu^2) \qquad (2)$$

which provides a linear interpolation between two charm densities at the scale μ^2, obtained at $w = w_{\rm max}$ and

$w = 0$. Later we will adopt the charm distribution function from the CTEQ66M set [39]. We will assume $w_{\max} = 3.5\%$, which corresponds to the CTEQ66c1 set [39]. Additionally, we have performed a three-point interpolation of the charmed quark distributions (for $w = 0\%$, $w = 1\%$ and $w = 3.5\%$, which correspond to the CTEQ66M, CTEQ66c0 and CTEQ66c1 sets, respectively). These results differ from the ones based on (2) by no more than 0.5%, thus giving confidence in our starting point [28]. Note that w in Eq. 2 is treated as a parameter which does not depend on μ^2. Therefore, its value can be determined from the fit to the data.

The general-purpose MC generator SHERPA [31] with leading order (LO) matrix elements (version 2.2.1) is used to generate samples for the extraction of the w from the ATLAS data.

The process $p+p \to \gamma+$ Heavy-Flavor(HF)-jet + up to 4 additional jets is simulated with the requirement $E_{\rm T}^{\gamma} > 20$ GeV. Additional cuts are applied to match the ATLAS event selection [30]. For the PDF we used CT14nnloIC included with the help of LHAPDF6 [40], which contains three *benchmark* w values (0%, 1%, 2%).

In order to extract the w-value from the data we first calculated the $E_{\rm T}^{\gamma}$-spectrum using the SHERPA MC generator in the central rapidity region ($|\eta^{\gamma}| < 1.37$).

Next, from the satisfactory description of the ATLAS data in the central rapidity region we have found the normalization coefficient $K = 1.95$. Then, using this scale factor we have fit the experimental $E_{\rm T}^{\gamma}$-spectrum in the forward rapidity region $1.56 \le |\eta^{\gamma}| < 2.37$ and $65 < E_{\rm T}^{\gamma} < 400$ GeV extracting, finally, the IC fraction $w = 1.14\%$. This procedure is illustrated by Fig. 1.

We have repeated the w-extraction procedure using the above-mentioned combined $k_{\rm T}$+collinear QCD factorization scheme instead of SHERPA, but without utilization of any normalization coefficient.

To calculate the $E_{\rm T}^{\gamma}$-spectrum in the forward rapidity region the CTEQ66c PDF was used, which includes the IC fraction in the proton. Then, we fit the experimental E_T^{γ}-spectrum as a function of w using a three-point interpolation of the charmed PDF. Finally, we determined the value of w which corresponds to the best description of the ATLAS data [30]. The scale uncertainties are shown by bands in Fig. 2. They are close to the scale uncertainties included by SHERPA (Fig. 1).

The w-dependence of χ^2-functions obtained with both SHERPA and the combined QCD approach are presented in Fig. 3. By definition, the minimum of the χ^2-function is reached at a central value $w_{\rm c}$ which corresponds to the best description of the ATLAS data. As already pointed above, the application of SHERPA results in $w_{\rm c} = 1.14\%$, and in the combined QCD gives us $w_{\rm c} = 1.00\%$.

Figure 3 shows a rather weak χ^2-sensitivity to the w-value. It is due to the large experimental and theoretical QCD scale uncertainties especially at $E_{\rm T}^{\gamma} > 100$ GeV (Figs. 1 and 2). Therefore it is not possible to extract the $w_{\rm c}$-value with a requested accuracy (3–5 σ), instead, we present relevant upper limits at different confidence levels in Table I.

The first line in Table I corresponds to the central value $w_{\rm c}$ obtained within two calculations, SHERPA and com-

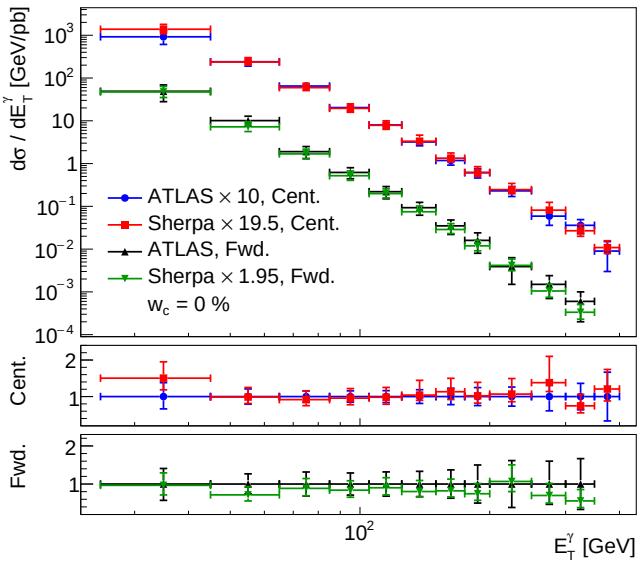

(a) $w_{\rm c} = 0\%$

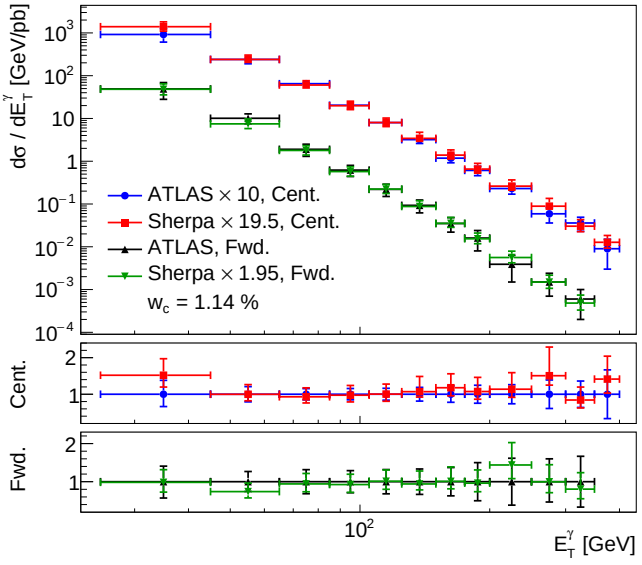

(b) $w_{\rm c} = 1.14\%$

FIG. 1. The $E_{\rm T}^{\gamma}$-spectrum calculated with MC generator SHERPA and multiplied by the factor $K = 1.95$ compared with the ATLAS data [30]. (a) top: the spectrum at the central rapidity region $|\eta^{\gamma}| < 1.37$ and forward $1.56 \le |\eta^{\gamma}| < 2.37$ region without the IC contribution; (a) middle: the ratio of the MC calculation to the data for the central rapidity region ($w = 0\%$); (a) bottom: the ratio of the MC calculation to the data for the for forward rapidity regions ($w = 0\%$). (b): the same spectra, as in (a), but with IC contribution $w = 1.14\%$ corresponded to the best fit of the data.

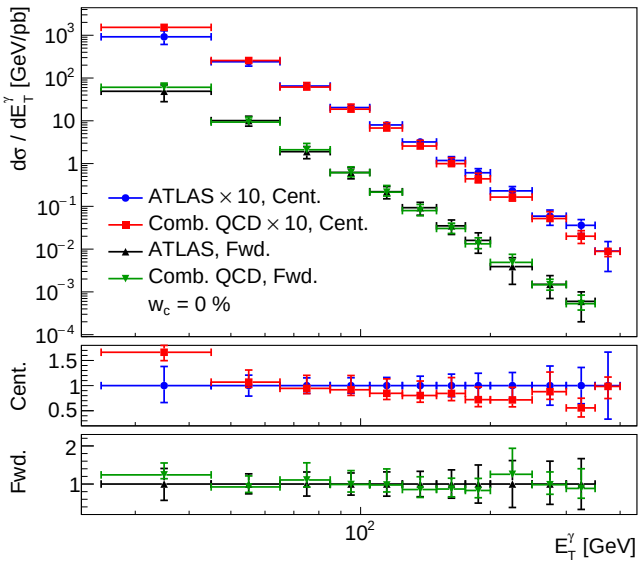

(a) $w_c = 0\%$

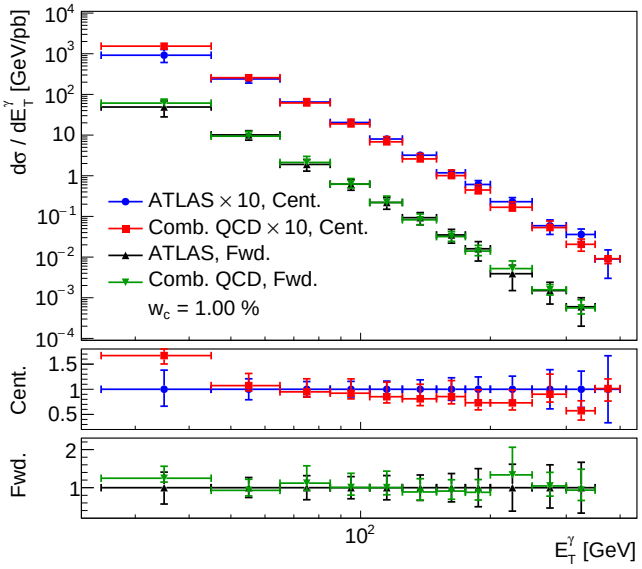

(b) $w_c = 1.00\%$

FIG. 2. The spectrum of prompt photons as a function of its transverse energy E_T^γ calculated with the combined QCD analysis, compared with ATLAS data [30]. (a) top: the spectrum in the central rapidity region $|\eta^\gamma| < 1.37$ and forward $1.56 \leq |\eta^\gamma| < 2.37$ region without the IC contribution; (a) middle: the ratio of the MC calculation to the data for the central rapidity region ($w = 0\%$); (a) bottom: the ratio of the MC calculation to the data for the forward rapidity regions ($w = 0\%$). (b): the same spectra, as in (a), but with IC contribution $w = 1.00\%$ corresponded to the best fit of the data.

bined QCD. The second (3rd, 4th) line gives w_c plus one (two, three) standard deviation(s), $w_{u.l.} = w_c + 1(2,3)\ \sigma$, which corresponds to 68% (90%, 95%) of the confidence level (C.L.). Even at a level of one standard deviation the w_c-value is comparable to $w = 0\%$, therefore it is

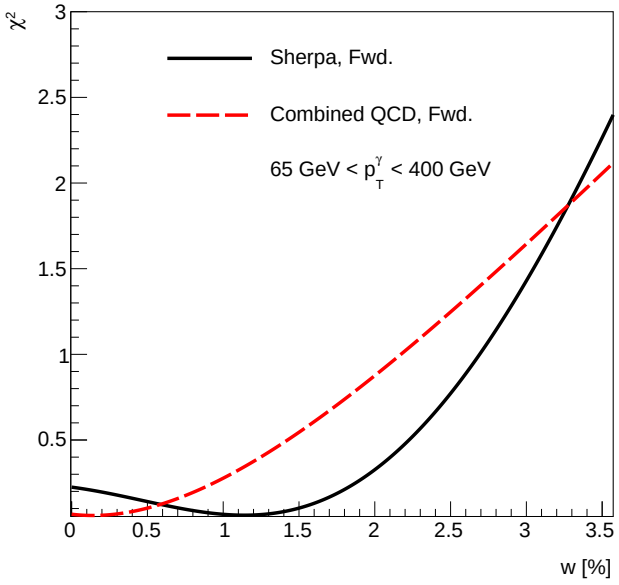

FIG. 3. Solid line: χ^2 as a function of w in the forward rapidity region in SHERPA. Dashed line: the similar χ^2 obtained by the combined QCD calculation.

	SHERPA [%]	Comb. QCD [%]
w_c	1.14	1.00
$w_{u.l.}$ (68% C.L.)	2.74	3.69
$w_{u.l.}$ (90% C.L.)	3.77	6.36
$w_{u.l.}$ (95% C.L.)	4.32	> 7.5

TABLE I. Central w_c value and upper limits $w_{u.l.}$ obtained within SHERPA and combined QCD calculations.

reasonable to indicate only the upper limit $w_{u.l.}$.

The combined QCD approach, in contrast to the SHERPA, allowed one to describe the data without any K-factor. Nevertheless, the SHERPA calculation is preferable for extraction of w value since the combined QCD approach predictions have larger theoretical uncertainties, especially at large transverse momenta (see Fig. 2). Therefore, the SHERPA upper limit $w_{u.l.} = 2.74\%$ (4.32%) at the 68% (95%) C.L. we consider as a most reliable one.

Note that the experimental error bars and the scale uncertainties calculated within the SHERPA program are similar whereas the scale uncertainties obtained using the combined QCD approach are much larger than the experimental uncertainties, as can be seen from Figs. 1, 2.

As a first estimate of the scale uncertainty we have used the conventional procedure, used in a literature, varying the values of the QCD renormalization scale μ_R and the factorization one μ_F in the interval from $0.5E_T^\gamma$ to $2E_T^\gamma$. In fact, there are several methods to check the sensitivity of observables to the scale uncertainty, see, for example, [41] and references there in. The renormalization scale uncertainty of the E_T^γ-spectra poses a serious theo-

retical problem for obtain a more precise estimate of the IC probability from the LHC data.

Note that the precision of IC probability estimation is limited by theoretical QCD scale uncertainties. For example, in the absence of these the upper limit $w_{\rm u.\,l.}$ could decrease about two times. Another limitation of $w_{\rm u.\,l.}$ comes from the systematic uncertainty of the measurement, which is mainly related to the light flavor jet tagging. Without these uncertainties one can reduce $w_{\rm u.\,l.}$ by comparable amount. In contrast to these uncertainties, statistical uncertainty doesn't play a large role. Therefore, to get more reliable information on the IC probability in proton from the next LHC data at $\sqrt{s} = 13$ TeV it is needed to do more realistic estimation of theoretical scale uncertainties and reduce systematic uncertainties.

This problem can be, in fact, eliminated by employing the "principle of maximum conformality" (PMC) [42] which sets renormalization scales by shifting the β terms in the pQCD series into the running coupling. The PMC predictions are independent of the choice of renormalization scheme — a key requirement of the renormalization group. Up to now there is no direct application of the PMC to the hard processes discussed in this paper. Therefore, its utilization will be the next step of our study.

In Fig. 4 our prediction on the distribution of prompt photons as a function of the transverse Feynman variable $x_{\rm T} = 2E^{\gamma}_{\rm T}/\sqrt{s}$ at $\sqrt{s} = 13$ TeV is presented at different IC probabilities $w = 0$, 1 and 2%. The ratio $IC\,/\,no\;IC$ presented in bottom of Fig. 4 shows that the inclusion of the IC contribution to PDF allows us to increase the yield of prompt photons about 1.5 times at $w = 1\%$ and about 3 times at $w = 2\%$ in the interval $0.12 < x_{\rm T} < 0.14$. At larger $x_{\rm T}$ values the statistics is very poor, therefore calculating $\mathrm{d}N/x_{\rm T}$-spectrum we are limited $x_{\rm T} \leq 0.14$. By the SHERPA calculation at $\sqrt{s} = 13$ TeV the following kinematical cuts were used: $0 \leq x_{\rm F} \leq 0.2$, $E^{\gamma}_{\rm T} \geq 100$ GeV, the integral luminosity $L = 100$ fb^{-1}, where $x_{\rm F} = 2p^{\gamma}_{\rm z}/\sqrt{s}$, $p^{\gamma}_{\rm z}$ is the longitudinal momentum of photon. According to our MC calculations, namely, these kinematical cuts available at ATLAS are preferable for observation of the IC signal in the $x_{\rm T}$-spectrum at $\sqrt{s} = 13$ TeV. Tests of $x_{\rm T}$-scaling and measurements of its distribution at different CM energies will provide new tests of intrinsic charm at the LHC.

In summary:

A first estimate of the intrinsic charm probability in the proton has been carried out utilizing recent ATLAS data on the prompt photon production accompanied by the c-jet at $\sqrt{s} = 8$ TeV [30]. To obtain more accurate results on the intrinsic charm contribution one needs additional data and at the same time reduced systematic uncertainty comming primarily from light jet tagging. In particular, very useful will be measurements of cross sections of $\gamma + c$ and $\gamma + b$ production in pp-collisions at $\sqrt{s} = 13$ TeV at high transverse momentum with high

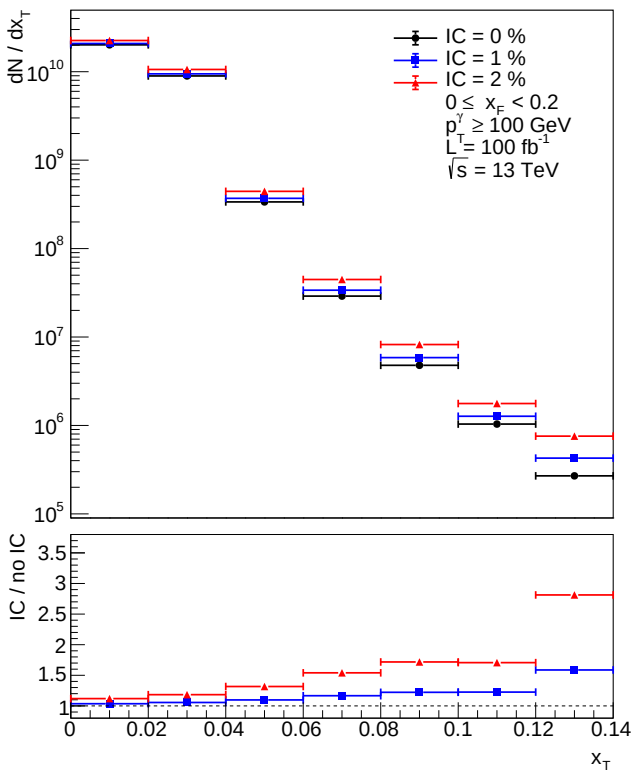

FIG. 4. Top: the distribution of number of prompt photon events as a function of $x_{\rm T}$ calculated within the MC generator SHERPA at $\sqrt{s} = 13$ TeV and different values of the IC probability $w = 0\%$ (circles), $w = 1\%$ (squares) and $w = 2\%$ (triangles). Bottom: the ratio of the MC calculation including the IC contribution and without it.

statistics [28]. The ratio of photon + charm to photon + bottom cross sections is very sensitive to the IC signal [28, 29]. The ratio, when $E^{\gamma}_{\rm T}$ grows, decreases in the absence of the IC contribution and stays flat or increases when the IC contribution is included. Furthermore, the measurements of $Z/W + c/b$ production in pp collision at 13 TeV could also give additional significant information on the intrinsic charm contribution [27, 29].

Acknowledgements

We thank A.A. Glasov, R. Keys, E.V. Khramov, S. Prince and S.M. Turchikhin for very helpful discussions. The authors are also grateful to S.P. Baranov, P.-H. Beauchemin, I.R. Boyko, Z. Hubacek, H. Jung, F. Hautmann, B. Nachman, P.M. Nadolsky, H. Tores and L. Rotali, N.A. Rusakovich for useful discussions and comments. The SHERPA calculations by J.S. were done at SIVVP (ERDF, ITMS 26230120002) computer cluster at Institute of Informatics, Slovak Academy of Sciences, J.S. is thankful for the opportunity of using this cluster. The work of A.V.L and M.A.M was supported in part by the grant of the President of Russian Federation NS-7989.2016.2. A.V.L. and M.A.M. are also grateful to DESY Directorate for the support in the framework

of Moscow — DESY project on Monte-Carlo implementation for HERA — LHC. M.A.M. was supported by a grant of the Foundation for the Advancement of Theoretical physics "Basis" 17-14-455-1 and RFBR grant 16-32-00176-mol-a. SJB is supported by the U.S. Department of Energy, contract DE–AC02–76SF00515.

* gennady.lykasov@cern.ch

[1] S. J. Brodsky, P. Hoyer, C. Peterson, and N. Sakai, Phys. Lett. **B93**, 451 (1980).
[2] S. J. Brodsky, J. C. Collins, S. D. Ellis, J. F. Gunion, and A. H. Mueller, in *ELECTROWEAK SYMMETRY BREAKING. PROCEEDINGS, WORKSHOP, BERKELEY, USA, JUNE 3-22, 1984* (1984).
[3] M. Franz, M. V. Polyakov, and K. Goeke, Phys. Rev. **D62**, 074024 (2000), arXiv:hep-ph/0002240 [hep-ph].
[4] B. W. Harris, J. Smith, and R. Vogt, Nucl. Phys. **B461**, 181 (1996), arXiv:hep-ph/9508403 [hep-ph].
[5] G. Bari *et al.*, Nuovo Cim. **A104**, 1787 (1991).
[6] F. G. Garcia *et al.* (SELEX), Phys. Lett. **B528**, 49 (2002), arXiv:hep-ex/0109017 [hep-ex].
[7] J. Badier *et al.* (NA3), Z. Phys. **C20**, 101 (1983).
[8] R. Vogt, S. J. Brodsky, and P. Hoyer, Nucl. Phys. **B360**, 67 (1991).
[9] S. J. Brodsky, S. Groote, S. Koshkarev, H. G. Dosch, and G. F. de Tramond, (2017), arXiv:1709.09903 [hep-ph].
[10] S. Barlag *et al.* (ACCMOR), Phys. Lett. **B247**, 113 (1990).
[11] G. I. Lykasov, G. H. Arakelian, and M. N. Sergeenko, Phys. Part. Nucl. **30**, 343 (1999), [Fiz. Elem. Chast. Atom. Yadra30,817(1999)].
[12] V. M. Abazov *et al.* (D0), Phys. Rev. Lett. **102**, 192002 (2009), arXiv:0901.0739 [hep-ex].
[13] V. M. Abazov *et al.* (D0), Phys. Lett. **B714**, 32 (2012), arXiv:1203.5865 [hep-ex].
[14] V. M. Abazov *et al.* (D0), Phys. Lett. **B719**, 354 (2013), arXiv:1210.5033 [hep-ex].
[15] T. Aaltonen *et al.* (CDF), Phys. Rev. **D81**, 052006 (2010), arXiv:0912.3453 [hep-ex].
[16] T. Aaltonen *et al.* (CDF), Phys. Rev. Lett. **111**, 042003 (2013), arXiv:1303.6136 [hep-ex].
[17] S. Rostami, A. Khorramian, A. Aleedaneshvar, and M. Goharipour, J. Phys. **G43**, 055001 (2016), arXiv:1510.08421 [hep-ph].
[18] A. Vafaee, A. Khorramian, S. Rostami, and A. Aleedaneshvar, *Proceedings, 18th High-Energy Physics International Conference in Quantum Chromodynamics (QCD 15): Montpellier, France, June 29-July 03, 2015*, Nucl. Part. Phys. Proc. **270-272**, 27 (2016).
[19] S. J. Brodsky, A. Kusina, F. Lyonnet, I. Schienbein, H. Spiesberger, and R. Vogt, Adv. High Energy Phys. **2015**, 231547 (2015), arXiv:1504.06287 [hep-ph].
[20] R. D. Ball *et al.* (NNPDF), JHEP **04**, 040 (2015), arXiv:1410.8849 [hep-ph].
[21] W. Freeman and D. Toussaint (MILC), Phys. Rev. **D88**, 054503 (2013), arXiv:1204.3866 [hep-lat].
[22] S. J. Brodsky and B.-Q. Ma, Phys. Lett. **B381**, 317 (1996), arXiv:hep-ph/9604393 [hep-ph].
[23] S. J. Brodsky and S. Gardner, Phys. Rev. **D65**, 054016 (2002), arXiv:hep-ph/0108121 [hep-ph].
[24] S. J. Brodsky, A. S. Goldhaber, B. Z. Kopeliovich, and I. Schmidt, Nucl. Phys. **B807**, 334 (2009), arXiv:0707.4658 [hep-ph].
[25] R. Laha and S. J. Brodsky, (2016), arXiv:1607.08240 [hep-ph].
[26] V. A. Bednyakov, M. A. Demichev, G. I. Lykasov, T. Stavreva, and M. Stockton, Phys. Lett. **B728**, 602 (2014), arXiv:1305.3548 [hep-ph].
[27] P.-H. Beauchemin, V. A. Bednyakov, G. I. Lykasov, and Yu. Yu. Stepanenko, Phys. Rev. **D92**, 034014 (2015), arXiv:1410.2616 [hep-ph].
[28] A. V. Lipatov, G. I. Lykasov, Yu. Yu. Stepanenko, and V. A. Bednyakov, Phys. Rev. **D94**, 053011 (2016), arXiv:1606.04882 [hep-ph].
[29] S. J. Brodsky, V. A. Bednyakov, G. I. Lykasov, J. Smiesko, and S. Tokar, Prog. Part. Nucl. Phys. **93**, 108 (2017), arXiv:1612.01351 [hep-ph].
[30] M. Aaboud *et al.* (ATLAS), (2017), arXiv:1710.09560 [hep-ex].
[31] T. Gleisberg, S. Hoeche, F. Krauss, M. Schonherr, S. Schumann, F. Siegert, and J. Winter, JHEP **02**, 007 (2009), arXiv:0811.4622 [hep-ph].
[32] L. V. Gribov, E. M. Levin, and M. G. Ryskin, Phys. Rept. **100**, 1 (1983).
[33] S. Catani, M. Ciafaloni, and F. Hautmann, Nucl. Phys. **B366**, 135 (1991).
[34] B. Andersson *et al.* (Small x), Eur. Phys. J. **C25**, 77 (2002), arXiv:hep-ph/0204115 [hep-ph].
[35] S. J. Brodsky, C. Peterson, and N. Sakai, Phys. Rev. **D23**, 2745 (1981).
[36] V. N. Gribov and L. N. Lipatov, Sov. J. Nucl. Phys. **15**, 438 (1972), [Yad. Fiz.15,781(1972)].
[37] G. Altarelli and G. Parisi, Nucl. Phys. **B126**, 298 (1977).
[38] Y. L. Dokshitzer, Sov. Phys. JETP **46**, 641 (1977), [Zh. Eksp. Teor. Fiz.73,1216(1977)].
[39] P. M. Nadolsky, H.-L. Lai, Q.-H. Cao, J. Huston, J. Pumplin, D. Stump, W.-K. Tung, and C. P. Yuan, Phys. Rev. **D78**, 013004 (2008), arXiv:0802.0007 [hep-ph].
[40] A. Buckley, J. Ferrando, S. Lloyd, K. Nordstrm, B. Page, M. Rfenacht, M. Schnherr, and G. Watt, Eur. Phys. J. **C75**, 132 (2015), arXiv:1412.7420 [hep-ph].
[41] X.-G. Wu, S. J. Brodsky, and M. Mojaza, Prog. Part. Nucl. Phys. **72**, 44 (2013), arXiv:1302.0599 [hep-ph].
[42] S. J. Brodsky, M. Mojaza, and X.-G. Wu, Phys. Rev. **D89**, 014027 (2014), arXiv:1304.4631 [hep-ph].